Binding Energies of Five Molecular Pincers Calculated by Explicit and Implicit Solvent Models

Jiří Kessler,*[a] Milan Jakubek,[b] Bohumil Dolenský,[b] and Petr Bouř*[a]

Molecular pincers or tweezers are designed to hold and release the target molecule. Potential applications involve drug distribution in medicine, environment technologies, or microindustrial techniques. Typically, the binding is dominated by van der Waals forces. Modeling of such complexes can significantly enhance their design; yet obtaining accurate complexation energies by theory is difficult. In this study, density functional theory (DFT) computations combined with dielectric continuum solvent model are compared with the potential of mean force approach using umbrella sampling and the weighted histogram analysis method (WHAM) with molecular dynamics (MD) simulations. For DFT, functional and basis set effects are discussed. The computed results are compared to experimental data based on NMR spectroscopic measurements of five synthesized tweezers based on the Tröger's basis. Whereas the DFT computations correctly provided the observed trends in complex stability, they failed to produce realistic magnitudes of complexation energies. Typically, the binding was overestimated by DFT if compared to experiment. The simpler semiempirical PM6-DH2X scheme proposed lately yielded better magnitudes of the binding energies than DFT but not the right order. The MD-WHAM simulations provided the most realistic Gibbs binding energies, although the approximate MD force fields were not able to reproduce completely the ordering of relative stabilities of model complexes found by NMR. Yet the modeling provides interesting insight into the complex geometry and flexibility and appears as a useful tool in the tweezers' design. © 2012 Wiley Periodicals, Inc.

DOI: 10.1002/jcc.23063

Introduction

Weakly bound molecular complexes attract attention as tools for molecular carriage, recognition, and manipulation.[1] The concept of molecular tweezers was introduced in 1978 by Chen and Whitlock[2] for compounds having two flat binding units connected by a linkage group. Typical tweezer compounds contain a rigid spacer and two aromatic residues. The aromatic parts attracts electron-deficient compounds.[3–5] For example, successful structural motifs included glycourils,[6,7] methanoantracenes,[8,9] and Kagan's ether.[10]

In the past, others and we proposed molecular tweezers based on oligo-Tröger's base (TB) derivatives.[11,12] The Tröger's base motif provides a convenient scaffold that can be easily modified by means of organic synthesis.[13–17]

Theoretical methods provide support to rationalize the synthesis of such compounds.[5,18–21] Realistic modeling of the affinity of the tweezers to the target molecule is of general interest, as similar weak intermolecular forces are found in molecular recognition, self-assembly, supramolecular chemistry, and general host–guest complexes.[22–24] Yet the binding process is quite complex and difficult to model. The weak ligand-tweezer forces, for example, include van der Waals (dispersion) interactions that are not included in conventional density functional theory (DFT) methods.[25,26] Fortunately, this seems to be overcome in the latest DFT approaches. Previously, we showed that also for the Tröger's tweezers Grimme's empirical correction[25,27] DFT energies do significantly improve the accuracy of DFT predictions of formation energies and other properties of the complexes.[28]

In this study, we compare the performance of implicit dielectric solvent models with molecular dynamics (MD) simulations based on explicit solvent involvement. The dielectric polarized continuum models (PCMs) used in quantum chemical (QC) methods respect the actual molecular shapes and provide reasonable estimates of solvation energies and changes of spectroscopic properties under solvation.[29–32] Conversely, the rigid dielectric environment is not always appropriate. For example, special PCM adaptations are required for computation of excited electronic states.[33,34] Also for vibrational properties of polar groups making hydrogen bonds to the solvent a limited performance of PCMs was observed.[35,36] Accounting for the MD and the temperature effects is usually possible only via single molecule partition function[37]; the gas phase approximation, however, may not be accurate enough for solutions. Finally, neither the solvent–solute dispersion interactions nor the dynamic competition of the ligand or solvent binding are by any means represented in PCM. Conversely, the PCM

[a] J. Kessler, P. Bouř
Department of Spectroscopy, Institute of Organic Chemistry and Biochemistry, Academy of Sciences, 166 10 Prague, Czech Republic
E-mail: kessler@uochb.cas.cz or bour@uochb.cas.cz
[b] M. Jakubek, B. Dolenský
Department of Analytical Chemistry, Institute of Chemical Technology, 166 28 Prague, Czech Republic

Contract/grant sponsor: Grant Agency of the Czech Republic; Contract/grant numbers: P208/11/0105 and P203/08/1445; Contract/grant sponsor: Ministry of Education of the Czech Republic; Contract/grant numbers: LH11033 and LM2010005.

models represent a convenient approximation of the solvent effects and molecular interaction in solution, as they allow to involve the solute at a high approximation level.[30,38–40]

All-atomic MD provides more rigorous means to estimate free (Gibbs) binding energies. MD simulations involve the solvent at the same computational level as the solute. Further environmental factors, such as temperature and pressure, can be varied. In the past, for example, we achieved a more faithful modeling of spectroscopic molecular properties by application of MD averaging than by PCMs.[41,42] But MD simulations are restricted by accuracy of the semiempirical force fields, and the computations can be quite lengthy for sizable systems. Other issues connected to accurate reproduction of binding energies by MD methods are reviewed in Ref. [43].

A principle problem is adequate sampling of the configuration space, which can be unreasonably lengthy for sizable molecules.[43,44] In this work, instead of analysis of an equilibrium system, we use the weighted histogram analysis method (WHAM)[44,45] that provides a more efficient and accurate determination of the binding energy. The method is a frequently used example of the potential of mean force (PMF) path approaches based on the umbrella sampling. The path approaches were shown to be superior to so called endpoint methods where individual energy contributions are estimated separately.[46] In this study, the MM/PBSA[47] (molecular mechanics/Poisson-Boltzmann surface area) endpoint method was also tested, and it provided results very close to those obtained by the WHAM analysis.

Although the MD/WHAM simulations became quite lengthy for the investigated molecules, the results convincingly indicated that the MD simulations are in the case of pincer systems more realistic than the static QC/PCM computations. Still, future improvement of the force field quality is desirable.

Methods

Experiment

The oligo-TBs **A**–**E** (Fig. 1) were prepared according the procedure described elsewhere.[11,48,49] Association constants (K) for complexes of TB with tetracyanobenzene (**TCB**) in chloroform solutions were obtained by a ^{1}H NMR titration[50] on the Varian Gemini spectrometer operating at 300 MHz.[28] **TCB** is often used as a model ligand for tweezer testing because its electrodeficient aromatic core stacks well with other aromates.[8] From K, we calculated the complex formation energies at the temperature $T = 300$ K as $\Delta G = -RT \ln(K)$, where R is the gas constant.

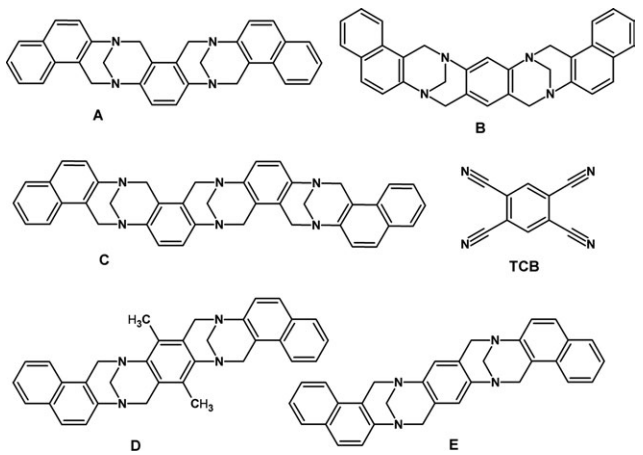

Figure 1. Studied tweezer molecules (**A–E**) and the **TCB** ligand.

Computations

Complexation energies for the reaction X + **TCB** → X**TCB**, where X = **A**-**E**, Figure 1, were calculated for fully optimized structures and complexes as $\Delta E = E_{\mathbf{XTCB}} - E_{\mathrm{X}} - E_{\mathbf{TCB}}$. Program Gaussian09[51] was used for the DFT/PCM computations. The BPW91[52] and B3LYP[53] functionals were used without and with the Grimme dispersion correction[25,27] (denoted as DFT-D or by the –D appendix to the functional) and standard Pople-style 6-31G, 6-31G**, 6-311G**, and 6-31++G** basis sets as implemented in Gaussian. The solvent was included as the PCM correction for chloroform. The Gaussian09 default integral equation formalism PCM parameters were used.[54] Within the BPW91 functional, the COSMO[55,56] (conductor-like solvent model) and SMD[57] (solvation models with solute electron density) models were tried as well. For estimation of zero-point energies, enthalpies, and Gibbs free energies, harmonic vibrational frequencies were calculated at the same level as for the optimization.

In addition, a newer reparameterized 'DFT-D3' variant[58] of the dispersion was estimated on single-point DFT-D geometries. The Turbomole program[59] was used for further MP2[60] and B3LYP[53] computations of equilibrium geometries and energies. Within Turbomole, the COSMO[55,56] solvent model was used instead of PCM. The impact of incomplete basis set was estimated by performing the counterpoise correction (cp)[61] on the complex geometries without further optimization.

Alternatively, the MOPAC2009 software[62] was used to estimate the binding energies, comprising the PM6[63] semiempirical method, the COSMO[55] model, and the PM6-DH2X correction[64] for van der Waals forces, hydrogen bonding, halogen–oxygen, and halogen–nitrogen interactions. For simplicity, we refer to the COSMO implementation in MOPAC2009 also as PCM, although the original COSMO theory forbade solvent polarizability.[65] We involve the PM6-DH2X method because it appeared recently[64] as an efficient tool for estimation of binding properties of weakly bond and biologically relevant complexes, providing results of nearly *ab initio* quality.[66]

For the explicit solvent modeling, one-dimensional WHAM procedure[44,45] was implemented in the Tinker[67] (our implementation). Alternatively, we used also an extension to the Amber[68] program (cf. http://membrane.urmc.rochester.edu/content/wham) to estimate binding free energies (ΔG) by the WHAM protocol. In Tinker and Amber, the MM3[69] and GAFF[70] (generalized Amber force field) force fields were used, respectively. For the WHAM analysis, we used the Amber program tools and our own scripts. The tweezer–**TCB** complex was placed in a cubic periodic box of $\sim$ 30 Å a side, and the dynamics was run with 1 fs integration time step and *NVT* thermodynamic ensemble, using temperature of 300 K. After an equilibration, a harmonic barrier (1 kcal/mol/Å^2) was applied to the tweezer–**TCB** distance (d_1, see Fig. 2 for definition), changed equidistantly within 6.9−11 Å (8.3−13.5 Å for **C**) and four (five for **C**) histograms were collected in Amber, each one for 100 ns MD run. In Tinker, which is

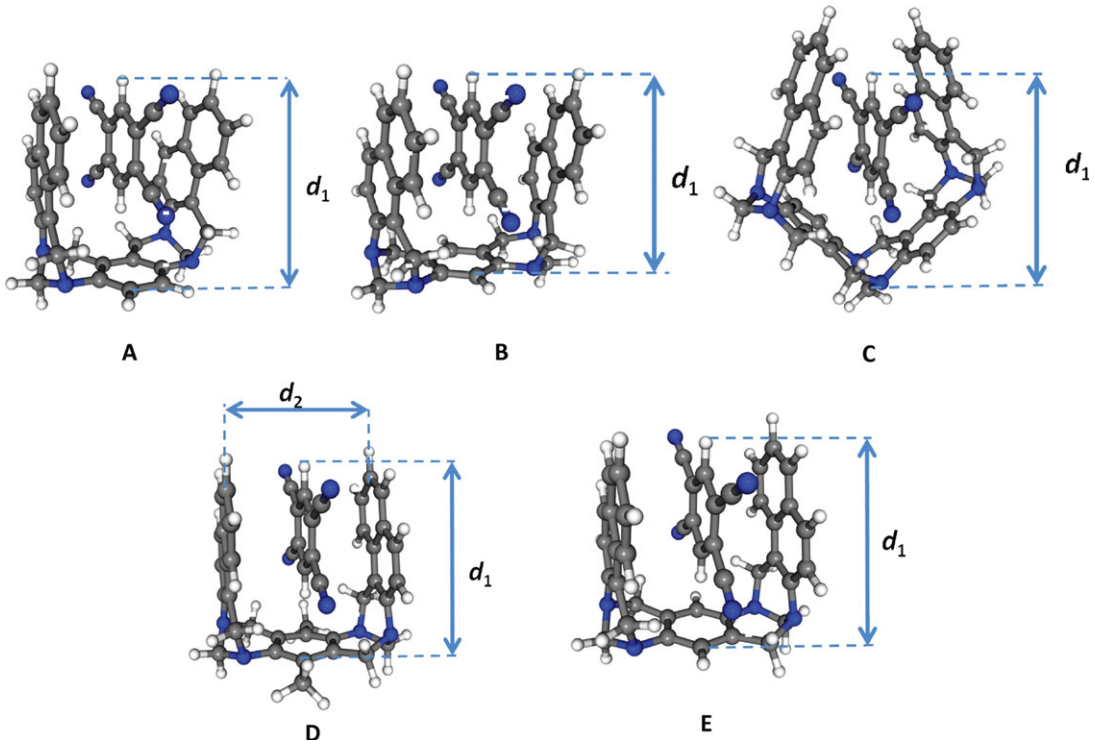

Figure 2. Lowest energy structures of the tweezer–**TCB** complexes calculated at the B3LYP-D/PCM/6-31G** level, and definition of the ligand-tweezer distances (d_1) and the tip dimension (d_2, displayed for **D** only). [Color figure can be viewed in the online issue, which is available at wileyonlinelibrary.com.]

computationally more demanding than Amber, 10 histograms of 1 ns runs were collected, within 6−18 Å for all complexes. This appeared sufficient for rough estimations of the MM3 and GAFF differences. Otherwise, the same parameters were used as for the Amber calculations.

Based on a 1 ns free dynamics run of the complex preformed in Amber, the binding energy was alternatively evaluated using the MM/PBSA[47] method. One thousand MD snapshot geometries were averaged, and the entropic part was calculated based on the normal mode analysis and $CHCl_3$ implicit solvent model as built in Amber.

Results and Discussion

PCM computations

From the comparison of the binding energies calculated for vacuum and chloroform represented by the PCM model in Table 1, we see that the dielectric solvent has a dramatic effect on complex stabilities for all the PM6, PM6-DH2X, and DFT methods, mostly weakening the binding by ∼5–10 kcal/mol. This can be to a large part explained by the quadrupole moment of the **TCB** ligand partially stabilized in the weakly polar chloroform environment.[8] The PM6 and PM6-DH2X semiempirical methods provide similar changes under solvation as the more advanced DFT (B3LYP-D/6-31G**) computation; the largest discrepancy occurs for compound **E** (e.g., ΔE_{PM6} = 5.8 kcal/mol vs. ΔE_{DFT} = 11.5 kcal/mol). However, although the solvent effects are similar for all the approaches, the absolute binding energies provided by DFT are about four times larger than those obtained by the empirical methods.

The DFT-D and DFT-D3 methods seem to provide very similar results. The DFT-D3 binding energies are on average by ∼10% higher; this might be caused, however, by the single-point geometry approximation. The differences in binding energies if calculated in vacuum and with the solvated model are very similar (DFT-D and DFT-D3 values differ less than 0.3 kcal/mol).

In Table 2, the electronic binding energies (ΔE), enthalpies (ΔH), and free energies (ΔG) obtained with several QC levels and the PCM, SMD, and COSMO ($CHCl_3$) solvent models are compared. For the energies, we see that although the PM6-DH2X semiempirical approach on average provides values (−0.5…−3.1 kcal/mol) reasonably close to the experimental ones (−1.7…−5.1 kcal/mol), the relative stability ordering is not so realistic as it does not correspond to the experimental trends. For example, the largest PM6-DH2X binding energy was predicted for the **C** complex, which was experimentally

Table 1. Binding energies ($\Delta E = E_{PCM} - E_{vac}$, kcal/mol) of the complexes in Figure 2 calculated in vacuum and chloroform.

	PM6		PM6-DH2X		DFT-D[a]		DFT-D3[a]	
Complex	E_{vac}	ΔE	E_{vac}	ΔE	E_{vac}	ΔE	E_{vac}	ΔE
A	−7.9	5.7	−7.3	6.2	−36.1	5.2	−40.1	5.3
B	−7.9	5.4	−6.0	5.5	−37.5	5.4	−41.0	5.3
C	−11.7	7.6	−10.8	7.7	−42.6	6.6	−46.2	6.4
D	−8.8	6.2	−8.0	6.4	−41.6	5.6	−45.4	5.6
E	−8.6	5.8	−7.8	6.0	−49.0	11.5	−51.9	11.2

[a] B3LYP-D/6-31G**.

Table 2. Binding electronic energies (ΔE), enthalpies (ΔH), and free energies (ΔG, all in kcal/mol) of the complexes (Fig. 2) calculated by several QC methods in the chloroform solvent.[a]

	ΔE							
Complex	DHX	B3LYP 6-31G** PCM	B3LYP-D 6-31G** PCM	B3LYP-D 6-31G** COSMO	B3LYP-D 6-31G**(cp) PCM	BPW91-D 6-31G** PCM	BPW91-D 6-31G** COSMO	BPW91-D 6-31G** SMD
A	−1.1	−2.7	−30.9	−31.3	−26.5	−24.8	−23.9	−18.1
B	−0.5	−3.3	−32.1	−32.5	−27.4	−26.5	−25.6	−19.9
C	−3.1	−10.7	−36.0	−35.9	−31.4	−28.7	−27.3	−22.4
D	−1.6	−4.0	−36.0	−36.6	−30.0	−30.3	−29.4	−22.6
E	−1.8	−4.1	−37.5	−38.0	−33.0	−31.9	−31.0	−24.6

	ΔE				ΔH	ΔG	
Complex	B3LYP-D 6-31++G** PCM	B3LYP-D 6-311G** PCM	MP2 6-31G** COSMO	MP2[b] 6-31G**(cp) COSMO	B3LYP-D 6-31G** PCM	B3LYP-D 6-31G** PCM	Exp.
A	−25.2	−28.7	−24.9	−13.8	−29.0	−13.5	−1.7
B	−26.2	−29.6	−27.0	−17.2	−30.0	−13.9	−2.8
C	−28.9	−32.8	−32.1	−20.5	−34.1	−18.5	−3.6
D	−29.6	−33.6	−33.8	−21.7	−34.1	−17.3	−3.9
E	−31.3	−40.9	−35.3	−23.7	−35.4	−18.7	−5.1

[a] The colors are introduced for easier orientation in calculated and experimental energy ordering (green—weakest complex, red—strongest binding, etc.). [Color table can be viewed in the online issue, which is available at wileyonlinelibrary.com.]

found much weaker than **E**. Conversely, the DFT-D methods do provide the experimental ordering of stabilities, with the BPW91 functional giving very similar results to B3LYP. The dispersion-uncorrected DFT binding energies (third column in Table 2) are several times smaller if compared to the DFT-D values, which is consistent with previous results, for example, tweezer nitrobenzene binding.[28] Significantly larger binding energies are obtained for **TCB** than for nitrobenzene, in agreement with the electrostatic concept[8] where the benzene ring in **TCB** is more electron-deficient than that in nitrobenzene, hence it is more attracted to the tweezer.

Despite the electrostatic attraction, the van der Waals dispersion forces are clearly dominant for the **TCB**–tweezer attraction, and the dispersion correction lowers the binding energies by ~30 kcal/mol. Conversely, the basis set variation has no effect on the relative energy ordering. Analogous basis set dependence was observed in vacuum and within PCM; therefore, we show the PCM results only. The smallest 6-31G basis is not included as it provided similar binding energies as 6-31G**. The 6-31G** → 6-31++G** change documented in Table 2 has a larger impact than 6-31G** → 6-311G**, which suggests that the diffuse functions (++) are more important then the σ-electrons for the intermolecular interaction and polarizabilities.

The effect of the basis set limitation can also be estimated from the counterpoise (cp) corrected energies. For the 6-31G** basis set, they are by about 4 and 10 kcal/mol smaller than the corresponding B3LYP-D and MP2 uncorrected values, respectively. For B3LYP-D, the relative ordering of **C** and **D** was switched by cp. Although due to the interference with the cavity used for the solvent model, the cp correction may not be so well justified as for vacuum, it indicates energy errors well comparable with the effect of the basis set changes (e.g., 6-31G** → 6-311G**). For our systems, the 6-31G** basis was the largest one that allowed us to compute the energies and vibrational properties of the complexes in a reasonable time for all the indicated approximation levels.

The MP2 results (Table 2) virtually copy the B3LYP-D/6-31G**/PCM values, as was also observed for similar systems in the past.[18,27,28] The COSMO model (as implemented in Turbomole, B3LYP-D) seems to provide almost the same binding energies as PCM (Gaussian), within ~1 kcal/mol. For the BPW91-D level, the PCM and COSMO models are compared to the SMD solvent approach. Using SMD leads to lowering of the predicted binding energies, typically by ~5 kcal/mol, in favor to the experimental results. This suggests that the solvent–solute dispersion interaction included in SMD[57] may be important for the correct description of the binding, which is further supported by the MD computations described below.

Within the QC/PCM approach, the temperature and vibrational dynamics corrections account for the discrepancies in the binding energy magnitudes only partially. The zero-point

Table 3. Binding free energies (ΔG, in kcal/mol) calculated by MD/WHAM with the GAFF and MM3 force fields, using the MM/PBSA model, and experiment.

Complex	GAFF	GAFF[a]	MM3	MM/PBSA	Exp.
A	−2.4	−1.8	−7.4	−5.5	−1.7
B	−0.4	−0.7	−4.8	−3.1	−2.8
C	−5.9	−0.7	−12.7	−9.9	−3.6
D	−2.1	−1.0	−8.5	−7.7	−3.9
E	−3.2	−1.1	−8.9	−8.0	−5.1

[a] **TCB** outside the cavity. [Color table can be viewed in the online issue, which is available at wileyonlinelibrary.com.]

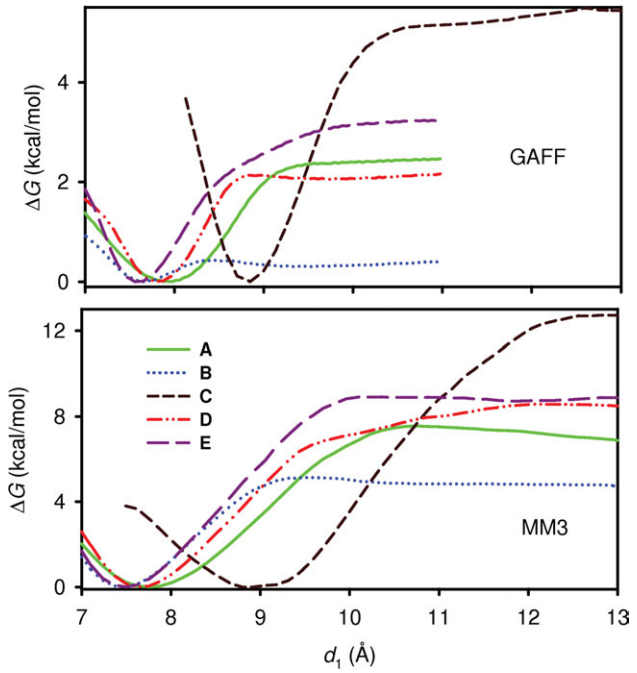

Figure 3. Free energy profiles for the tweezer–**TCB** complexes obtained by the weighted histogram analysis method from the Amber (top, GAFF force field) and Tinker (bottom, MM3 force field) dynamics.

energies (not shown) and enthalpies (ΔH, Table 2) differ from the energies by about 1–2 kcal/mol only. Conversely, the Gibbs free energies (ΔG) dramatically deviate from the electronic energies or enthalpies, being mostly smaller in absolute values by ~50%, and thus much closer to experiment. This suggests a large entropic contribution to complex stabilities. Nevertheless, such QC free energies are still rather large if compared to the observations. Additionally, the QC estimation of the partition function based on an isolated molecule model may not be quite adequate for our system, and the continuum solvent models may miss important interaction and dynamics components.

MD results

Indeed, the MD simulations provide the most faithful representation of the complexation experiments. The binding free energies calculated by WHAM (Table 3) are reasonably close to experiment and approximately follow the experimental relative stability ordering. The GAFF seems to provide better results than the MM3 force field, the latter giving binding energies 2–3× larger. Note, however, that the MD/WHAM procedure is by an order computationally more demanding (~1.5 years were needed for the results presented, if recalculated to a 2 GHz 64 bit processor) than the static DFT computations (~weeks–months).

It is interesting that relatively large binding energies are obtained for **TCB** bound to the tweezers outside the cavity; for **B**, the out of cavity binding energy (−1.0 kcal/mol) is even more favorable than in cavity binding (−0.4 kcal/mol). Mostly, however, the cavity binding is preferred and provides a better representation of the stability ordering if compared to experiment. We do not consider the outside cavity binding to be probable as other computations (DFT-D, not shown) predict that the outside binding energy is less than 50% of the cavity binding one, and no available experimental experience suggests it. Therefore, the GAFF result for **B** can be most probably explained by the inaccuracy of the MD force field.

The MM/PBSA energies (fifth column in Table 3) are consistent with the MD/WHAM results and closer to those obtained with the MM3 force field than for GAFF. The MM/PBSA procedure with implicit solvent model for chloroform thus appears as a computationally cheaper alternative to the more rigorous WHAM methods. Previously, similar encouraging results by MM/PBSA were obtained for biological models in aqueous environment.[46,47,71]

The full PMF profiles obtained by the WHAM analysis with the GAFF and MM3 force fields are plotted in Figure 3. Both force fields provide similar shapes of the potential wells for all the complexes, although MM3 yields a more uniform dispersion of the equilibrium distances than GAFF (~7.5–7.7 Å vs. 7.5–8.0 Å for **A**, **B**, **D**, and **E**). The MM3/Tinker binding energies are also more uniform and larger than those obtained by GAFF/Amber (cf. Table 3). This suggests that the MM3 force field is not refined enough to discriminate between subtle changes in the TB structures. For **C**, similar equilibrium distance (d_1 ~8.8 Å) is obtained by both methods. Conversely, the MM3 binding potential wells are wider. From the energy profiles in Figure 3, it is apparent that there is no activation barrier for **TCB** to overcome while escaping the cavity.

The potential wells inside the cavity (Fig. 3) are mostly deeper than those for the outside cavity binding (Fig. 4). Outside, the **TCB**–tweezer interaction is less specific than for the cavity binding; all the **A**–**C** compounds provide rather similar curves (Fig. 4). When the distance increases over ~6 Å, an attractive potential is not apparent any more, as corresponds to the short-distance r^{-6} dispersion and electric quadrupole interaction terms. A weak barrier at 6−7 Å calculated in this direction (d_3, Fig. 4) suggests that the ligand **TCB** needs to

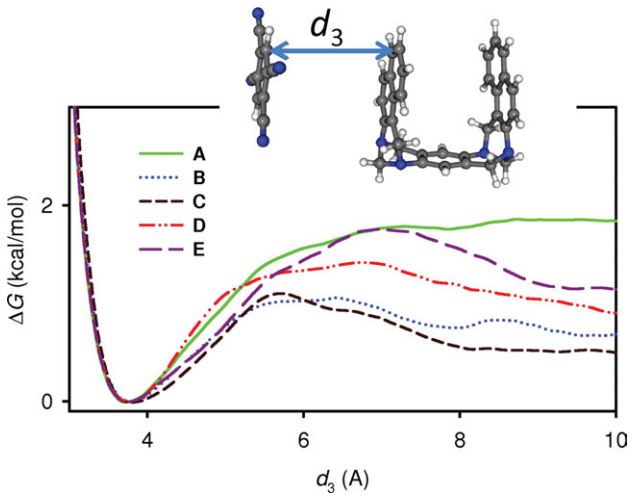

Figure 4. Outside cavity binding, free energy profile obtained by the GAFF/WHAM (10 histograms with 10 millions steps) dynamics with respect to the distance d_3.

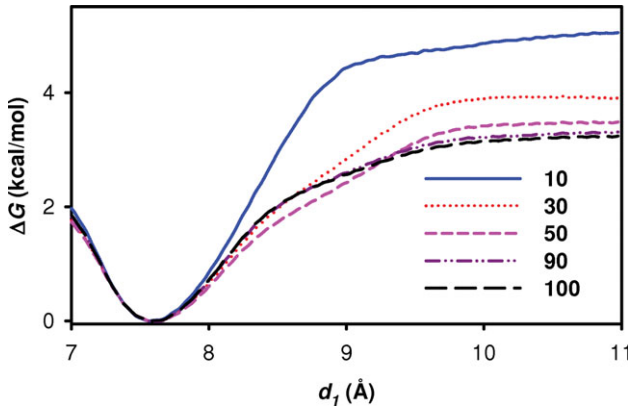

Figure 5. Convergence of the PMF WHAM/GAFF potential, for the **E** complex; millions of MD steps are indicated. [Color figure can be viewed in the online issue, which is available at wileyonlinelibrary.com.]

overcome a solvation shell or and electrostatic force to realize the binding.

It should be noted that the accuracy in the binding energies may be affected by the limited box size; however, this uncertainty is smaller than the differences between the studied compounds. To test other numerical errors, we performed several WHAM computations with 10, 30, 50, 90, and 100 millions of MD steps. As documented for the **E** complex in Figure 5 with the PMF potentials. The default 100 million steps appear as a reasonably converged limit. Thus, the force field inaccuracy is probably the most limiting factor in the MD simulations. Indeed, the MM3/GAFF differences in Table 3, for example, are much larger than the numerical variations.

Table 4. The complex and tweezer d_1 and d_2 distances (in Å, see Fig. 2) calculated by the DFT-D and MD WHAM methods.

	Compound				
	A	**B**	**C**	**D**	**E**
B3LYP-D/6-31G**/PCM($CHCl_3$)					
d_1	7.9	7.5	9.0	7.4	7.3
d_2	6.7	6.4	4.6	6.9	6.9
GAFF					
d_1	7.9	7.8	9.3	7.7	7.6
d_2	8.3	8.9	5.7	8.3	7.6
$<\Delta d_1>$[a]	0.4	0.4	0.2	0.4	0.3
$<\Delta d_2>$[a]	1.1	1.3	0.4	1.4	0.7

[a] Standard deviations from a 2 ns MD run.

Geometry parameters

In Table 4, the d_1 and d_2 characteristic distances (Fig. 1) are listed as calculated by the DFT-D and MD/GAFF approaches. For comparable molecules (**A**, **B**, **D**, and **E**) the d_2 molecular tip distances are quite similar, but DFT-D provides smaller values (6.4–6.9 Å) than MD (7.6–8.9 Å). The dynamically averaged tweezers are more opened. The dimensions do not exhibit any correlation with the complex stability. For MD, this can be understood from the large standard deviations ($<\Delta d_2> =$ 0.4−1.4 Å, Table 4) allowing the ligand to enter and leave the cavity comfortably.

Similarly, minor differences are apparent for the **TCB**–tweezer distances d_1. Note that for consistency with the WHAM calculations, the distance is defined as between the **TCB** most distant hydrogen and the center of the tweezer benzene ring (Fig. 2). The smaller d_1 distances for **D** and **E**, as

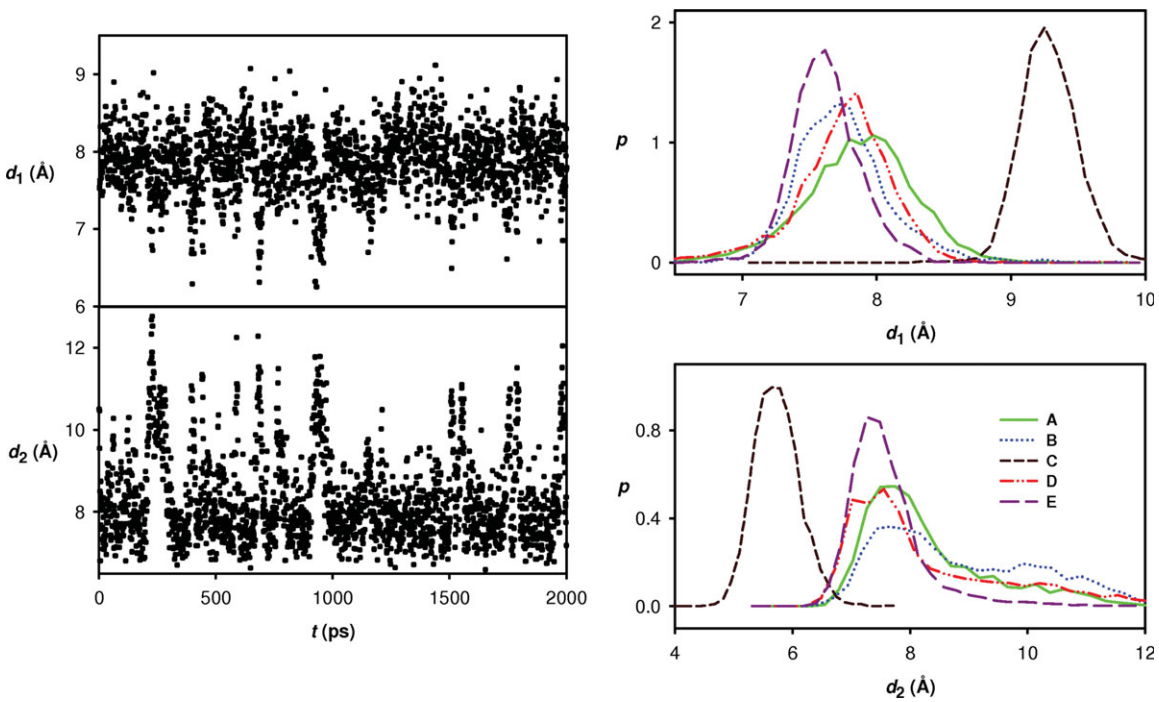

Figure 6. (Left) selected d_1 and d_2 distances for compound A within the Amber/GAFF 2 ns dynamics, and (right) the resultant probability distributions. [Color figure can be viewed in the online issue, which is available at wileyonlinelibrary.com.]

opposed to **A** and **B**, inversely correlate with the stability of the complexes. In the "bis" compounds (with respect to the number of the Tröger's units, **A**, **B**, **D**, and **E**), the deviation Δd_1 is smaller than in the "tris" complex **C**, which is closed more. The capping in **C** thus significantly restricts the ligand, but this is apparently not accompanied by increased complex stability (cf. Tables 2 and 3).

The dynamical behavior is documented in more detail in Figure 6, where the probability distributions of the d_1 and d_2 dimensions are plotted as obtained from a restrain-free Amber/GAFF 2 ns dynamics. The computationally most strongly binding bis compound **E** exhibits the narrowest d_1-distribution, whereas a weak, but not the weakest, binder **A** provides the broadest distribution. The molecular flexibility and consequent entropic contribution thus appears as a significant factor in the complex stability. The stochastic character of the temporal dependence of d_1 and d_2 is documented on the left hand side of Figure 6 for complex **A**. Occasional tweezer opening (d_2) or **TCB** depart (d_1) suggests a good equilibration and a strong interaction with the solvent. However, a close look reveals longer time (~0.5 ns/period) oscillation, most probably stemming from the structural rearrangements of the solvation shell, which makes the simulations very time-consuming.

Conclusions

To estimate applicability of various theoretical approaches for rational design of tweezer molecules of specific binding properties, we investigated the complexation of five typical compounds with the **TCB** ligand. Experimentally, the binding constants and the free binding energies were determined by NMR titration. The energies were also reproduced by computations using the static QC-PCM/COSMO models, molecular dynamic simulations coupled with the PMF/WHAM analysis, and the MM/PBSA method.

From the several QC approaches used, the B3LYP functional if corrected for the dispersion interactions provided the most realistic relative complex stabilities, although the binding energies were significantly overestimated. The overestimation could be only partially removed by calculating of the free energies (ΔG) based on the one-molecule model. The PM6 and PM6-DH2X semiempirical methods provided lower and more realistic magnitudes of binding energies than DFT, in favor to experiment, but failed to reproduce the experimental energy ordering.

The MD simulations thus appear as a more realistic approach. The MD-PMF/WHAM complexation energies were closer to experiment than for DFT, and the most important trends in complex stability were retained. However, occasionally, the MD relative stability ordering was switched, if compared to DFT and experiment. The GAFF force field implemented in Amber provided better results in shorter computational time than the MM3 approximation in the Tinker program.

The results document that the precision of the theoretical methods starts to be sufficient for practical prediction of reactivities and stabilities of such relatively complicated molecular systems.

Keywords: molecular tweezers · density functional theory · molecular dynamics · weighting histogram analysis method · dispersion forces · Tröger's base · solvent modeling

How to cite this article: J. Kessler, M. Jakubek, B. Dolenský, P. Bouř, *J. Comput. Chem.* **2012,** *33,* 2310–2317. DOI: 10.1002/jcc.23063

[1] J. L. Atwood, J. W. Steed, Supramolecular Chemistry; Wiley: Weinheim, **2000**.
[2] C. W. Chen, H. W. Whitlock, *J. Am. Chem. Soc.* **1978**, *100,* 4921.
[3] S. C. Zimmerman, *Top. Curr. Chem.* **1993**, *165,* 71.
[4] M. Hardouin-Lerouge, P. Hudhomme, M. Salle, *Chem. Soc. Rev.* **2011**, *40,* 30.
[5] Y. Chang, Y. Chen, C. Chen, Y. Wen, J. Lin, H. Chen, M. Kuo, I. Chao, *J. Org. Chem.* **2008**, *73,* 4608.
[6] J. W. H. Smeets, R. P. Sijbesma, F. G. M. Niele, A. L. Spek, W. J. J. Smeets, R. J. M. Nolte, *J. Am. Chem. Soc.* **1987**, *109,* 928.
[7] A. E. Rowan, J. A. A. W. Elemans, R. J. M. Nolte, *Acc. Chem. Res.* **1999**, *32,* 995.
[8] F. G. Klärner, B. Kahlert, A. Nellesen, J. Zienau, C. Ochsenfeld, T. Schrader, *J. Am. Chem. Soc.* **2006**, *128,* 4831.
[9] P. Talbiersky, F. Bastkowski, F. G. Klärner, T. Schrader, *J. Am. Chem. Soc.* **2008**, *130,* 9824.
[10] M. Harmata, *Acc. Chem. Res.* **2004**, *37,* 862.
[11] M. Valík, B. Dolenský, H. Petříčková, V. Král, *Collect. Czech. Chem. Commun.* **2002**, *67,* 609.
[12] C. Pardo, E. Sesmilo, E. Gutierrez-Puebla, A. Monge, J. Elquero, A. J. Fruchier, *J. Org. Chem.* **2001**, *66,* 4104.
[13] B. Dolenský, J. Elquero, V. Král, C. Pardo, M. Valík, *Adv. Heterocycl. Chem.* **2007**, *93,* 1.
[14] S. Sergeyev, *Helv. Chim. Acta* **2009**, *92,* 415.
[15] B. Dolenský, V. Parchaňský, P. Matějka, M. Havlík, P. Bouř, V. Král, *J. Mol. Struct.* **2011**, *996,* 69.
[16] M. Havlík, V. Parchaňský, P. Bouř, V. Král, B. Dolenský, *Collect. Czech. Chem. Commun.* **2009**, *74,* 1091.
[17] M. Valík, P. Matějka, E. Herdtweck, V. Král, B. Dolenský, *Collect. Czech. Chem. Commun.* **2006**, *71,* 1278.
[18] M. P. Waller, H. Kruse, C. Mück-Lichtenfeld, S. Grimme, *Chem. Soc. Rev.* **2012**, *41,* 3119.
[19] W. L. Jorgensen, D. L. Severance, *J. Am. Chem. Soc.* **1990**, *112,* 4768.
[20] C. Ochsenfeld, J. Kussmann, F. Koziol, *Angew. Chem. Int. Ed. Engl.* **2004**, *43,* 4485.
[21] G. F. Klarner, J. Panitzky, D. Preda, L. T. Scott, *J. Mol. Model.* **2000**, *6,* 318.
[22] C. A. Hunter, J. K. M. Sanders, *J. Am. Chem. Soc.* **1990**, *112,* 5525.
[23] A. Stone, The Theory of Intermolecular Forces; Oxford University Press: Oxford, **1997**.
[24] J. Šponer, P. Hobza, *Collect. Czech. Chem. Commun.* **2003**, *68,* 2231.
[25] S. Grimme, *J. Comput. Chem.* **2004**, *25,* 1463.
[26] J. Černý, P. Hobza, *Phys. Chem. Chem. Phys.* **2005**, *7,* 1624.
[27] S. Grimme, *J. Comput. Chem.* **2006**, *27,* 1787.
[28] V. Parchaňský, P. Matějka, B. Dolenský, M. Havlík, P. Bouř, *J. Mol. Struct.* **2009**, *934,* 117.
[29] S. Corni, C. Cappelli, R. Cammi, J. Tomasi, *J. Phys. Chem. A* **2001**, *105,* 8310.
[30] L. Gontrani, B. Mennucci, J. Tomasi, *J. Mol. Struct. (THEOCHEM)* **2000**, *500,* 113.
[31] R. Cammi, B. Mennucci, J. Tomasi, *J. Phys. Chem. A* **2000**, *104,* 5631.
[32] M. Cossi, V. Barone, R. Cammi, J. Tomasi, *Chem. Phys. Lett.* **1996**, *255,* 327.
[33] M. Caricato, B. Mennucci, J. Tomasi, F. Ingrosso, R. Cammi, S. Corni, G. Scalmani, *J. Chem. Phys.* **2006**, *124,* 124520.

[34] M. Caricato, F. Ingrosso, B. Mennucci, J. Tomasi, *J. Chem. Phys.* **2005**, *122,* 154501.
[35] P. Bouř, D. Michalík, J. Kapitán, *J. Chem. Phys.* **2005**, *122,* 144501.
[36] P. Bouř, *J. Chem. Phys.* **2004**, *121,* 7545.
[37] D. A. McQuarrie, Statistical Thermodynamics; Harper and Row: New York, **1973**.
[38] B. Mennucci, C. Cappelli, R. Cammi, J. Tomasi, *Chirality* **2011**, *23,* 717.
[39] B. Mennucci, E. Cancès, J. Tomasi, *J. Phys. Chem. B* **1997**, *101,* 10506.
[40] J. Tomasi, M. Persico, *Chem. Rev.* **1994**, *94,* 2027.
[41] K. H. Hopmann, K. Ruud, M. Pecul, A. Kudelski, M. Dračínský, P. Bouř, *J. Phys. Chem. B* **2011**, *115,* 4128.
[42] M. Dračínský, J. Kaminský, P. Bouř, *J. Phys. Chem. B* **2009**, *113,* 14698.
[43] M. K. Gilson, J. A. Given, B. L. Bush, J. A. McCammon, *Biophys. J.* **1997**, *72,* 1047.
[44] S. Kumar, D. Bouzida, R. H. Swendsen, P. A. Kollman, J. M. Rosenberg, *J. Comput. Chem.* **1992**, *13,* 1011.
[45] B. Roux, *Comput. Phys. Commun.* **1995**, *91,* 275.
[46] M. S. Lee, M. A. Olson, *Biophys. J.* **2006**, *90,* 864.
[47] P. Kollman, I. Massova, C. Reyes, B. Kuhn, S. Huo, L. Chong, M. Lee, T. Lee, Y. Duan, W. Wang, O. Donini, P. Cieplak, J. Srinivasan, D. Case, T. E. Cheatham, *Acc. Chem. Res.* **2000**, *33,* 889.
[48] J. Artacho, P. Nilsson, K. E. Bergquist, O. F. Wendt, K. Wärnmark, *Chem. Eur. J.* **2006**, *12,* 2692.
[49] M. Havlík, V. Král, B. Dolenský, *Org. Lett.* **2006**, *8,* 4867.
[50] C. Schalley, Analytical Methods in Supramolecular Chemistry; Wiley-VCH, **2007**.
[51] M. J. Frisch, G. W. Trucks, H. B. Schlegel, G. E. Scuseria, M. A. Robb, J. R. Cheeseman, G. Scalmani, V. Barone, B. Mennucci, G. A. Petersson, H. Nakatsuji, M. Caricato, X. Li, H. P. Hratchian, A. F. Izmaylov, J. Bloino, G. Zheng, J. L. Sonnenberg, M. Hada, M. Ehara, K. Toyota, R. Fukuda, J. Hasegawa, M. Ishida, T. Nakajima, Y. Honda, O. Kitao, H. Nakai, T. Vreven, J. Montgomery, J. A., J. E. Peralta, F. Ogliaro, M. Bearpark, J. J. Heyd, E. Brothers, K. N. Kudin, V. N. Staroverov, R. Kobayashi, J. Normand, K. Raghavachari, A. Rendell, J. C. Burant, S. S. Iyengar, J. Tomasi, M. Cossi, N. Rega, J. M. Millam, M. Klene, J. E. Knox, J. B. Cross, V. Bakken, C. Adamo, J. Jaramillo, R. Gomperts, R. E. Stratmann, O. Yazyev, A. J. Austin, R. Cammi, C. Pomelli, J. W. Ochterski, R. L. Martin, K. Morokuma, V. G. Zakrzewski, G. A. Voth, P. Salvador, J. J. Dannenberg, S. Dapprich, A. D. Daniels, O. Farkas, J. B. Foresman, J. V. Ortiz, J. Cioslowski, D. J. Fox; Gaussian 09, Revision A02, Gaussian, Inc.: Wallingford CT, **2009**.
[52] A. Becke, *Phys. Rev. A* **1988**, *38,* 3098.
[53] A. D. Becke, *J. Chem. Phys.* **1993**, *98,* 5648.
[54] G. Scalmani, M. J. Frisch, *J. Chem. Phys.* **2010**, *132,* 114110.
[55] A. Klamt, V. Jonas, T. Burger, J. C. W. Lohrentz, *J. Phys. Chem. A* **1998**, *102,* 5074.
[56] A. Klamt. In The Encyclopedia of Computational Chemistry; P. R. Schleyer, N. L. Allinger, T. Clark, J. Gasteiger, P. A. Kollman, H. F. Schaefer, III, P. R. Schreiner, Eds.; Wiley: Chichester, **1998**, p. 604.
[57] A. V. Marenich, C. J. Cramer, D. G. Truhlar, *J. Phys. Chem. B* **2009**, *113,* 6378.
[58] S. Grimme, J. Antony, S. Ehrlich, H. Krieg, *J. Chem. Phys.* **2010**, *132,* 154104.
[59] R. Ahlrichs, M. Bar, H.-P. Baron, R. Bauernschmitt, S. Bocker, M. Ehrig, K. Eichkorn, S. Elliot, F. Furche, F. Haase, M. Haser, H. Horn, C. Huber, U. Huniar, M. Kattannek, C. Kolmel, M. Koolwitz, K. May, C. Ochsenfeld, H. Ohm, A. Schafer, U. Schneider, O. Treutler, M. von Arnim, F. Weigend, P. Weis, H. Weiss, Quantum Chemistry Group; University of Karlsruhe: Karlsruhe, **1998**.
[60] C. Møller, M. S. Plesset, *Phys. Rev.* **1934**, *46,* 618.
[61] S. F. Boys, F. Bernardi, *Mol. Phys.* **1970**, *19,* 553.
[62] J. J. P. Steward; Steward Computational Chemistry: Colorado Springs, **2008**.
[63] J. J. P. Steward, *J. Mol. Modeling* **2007**, *13,* 1173.
[64] P. Dobeš, J. Řezáč, J. Fanfrlík, M., Otyepka, P. Hobza, *J. Phys. Chem. B.* **2011**, *115,* 8581.
[65] A. Klamt, G. Schuurmann, *J. Chem. Soc. Perkin Trans.* **1993**, *2,* 799.
[66] J. Řezáč, P. Hobza, *J. Chem. Theory Comput.* **2012**, *8,* 141.
[67] J. W. Ponder; Washington University School of Medicine: Saint Louis, **2000**.
[68] D. A. Pearlman, D. A. Case, J. W. Caldwell, W. S. Ross, T. E. Cheatham, S. Debolt, D. M. Ferguson, G. Seibel, P. A. Kollman, *Comput. Phys. Commun.* **1995**, *91,* 1.
[69] J. H. Lii, N. L. Allinger, *J. Am. Chem. Soc.* **1989**, *111,* 8576.
[70] J. Wang, R. M. Wolf, J. W. Caldwell, P. A. Kollman, D. A. Case, *J. Comput. Chem.* **2005**, *25,* 1157.
[71] B. Kuhn, P. Gerber, T. Schulz-Gasch, M. Stahl, *J. Med. Chem.* **2005**, *48,* 4040.

Received: 7 March 2012
Revised: 20 June 2012
Accepted: 21 June 2012
Published online on 10 July 2012